
RFLPA: A Robust Federated Learning Framework against Poisoning Attacks with Secure Aggregation

Peihua Mai

National University of Singapore
peihua.m@u.nus.edu

Ran Yan

National University of Singapore
e0709174@u.nus.edu

Yan Pang *

National University of Singapore
bizpyj@nus.edu.sg

Abstract

Federated learning (FL) allows multiple devices to train a model collaboratively without sharing their data. Despite its benefits, FL is vulnerable to privacy leakage and poisoning attacks. To address the privacy concern, secure aggregation (SecAgg) is often used to obtain the aggregation of gradients on sever without inspecting individual user updates. Unfortunately, existing defense strategies against poisoning attacks rely on the analysis of local updates in plaintext, making them incompatible with SecAgg. To reconcile the conflicts, we propose a robust federated learning framework against poisoning attacks (RFLPA) based on SecAgg protocol. Our framework computes the cosine similarity between local updates and server updates to conduct robust aggregation. Furthermore, we leverage verifiable packed Shamir secret sharing to achieve reduced communication cost of $O(M + N)$ per user, and design a novel dot-product aggregation algorithm to resolve the issue of increased information leakage. Our experimental results show that RFLPA significantly reduces communication and computation overhead by over 75% compared to the state-of-the-art method, BREA, while maintaining competitive accuracy.

1 Introduction

Federated learning (FL) is a promising machine learning technique that has been gaining attention in recent years. It enables numerous devices to collaborate on building a machine learning model without sharing their data with each other [33]. Compared with traditional centralized machine learning, FL preserves the data privacy by ensuring that sensitive data remains on local devices.

Despite its benefits, FL still has two key concerns to be addressed. Firstly, there is a threat of privacy leakage from local update. Recent works have demonstrated that the individual updates could reveal sensitive information, such as properties of the training data [34, 16], or even allows the server to reconstruct the training data [44, 12]. The second issue is that FL is vulnerable to poisoning attacks. Indeed, malicious users could send manipulated updates to corrupt the global model at their will [3]. The poisoning attacks may degrade the performance of the model, in the case of *untargeted attacks*, or bias the model's prediction towards a specific target labels, in the case of *targeted attacks* [20].

Secure aggregation (SecAgg) has become a potential solution to address the privacy concern. Under SecAgg protocol, the server could obtain the sum of gradients without inspecting individual user updates [9, 4]. However, the protocol poses a significant challenge in resisting poisoning attacks in

*Correspondence author

FL. Most defense strategies [8, 11] require the server to access local updates to detect the attackers, which increases the risk of privacy leakage. The contradiction makes it difficult to develop a FL framework that simultaneously resolves the privacy and robustness concerns.

To our best knowledge, BREa is the first FL framework that defends against poisoning attacks using SecAgg protocol [41]. Based on verifiable secret sharing, their framework leveraged the pairwise distances to remove outliers. However, their work is limited by the scaling concerns arising from computation and communication complexity. For a model with dimension M and N selected clients, the framework incurs $O(MN + N)$ communication per user, and $O((N^2 + MN) \log^2 N \log \log N)$ computation for the server due to the costly aggregation rule. Furthermore, BREa made unrealistic assumptions that the users could establish direct communication channels with other mobile devices.

To address the above challenge, we propose a robust federated learning framework against poisoning attacks (RFLPA) based on SecAgg protocol. We leverage verifiable packed Shamir secret sharing to compute the cosine similarity and aggregate gradients in a secure manner with reduced communication cost of $O(M + N)$ per user. To resolve the increased information leakage from packed secret sharing, we design a dot product aggregation protocol that only reveals a single value of the dot product to the server. Our framework requires the server to store a small and clean root dataset as the benchmark. Each user relies on the server to communicate the secret with each other, and utilizes encryption and signature techniques to ensure the secrecy and integrity of messages.

Our main contributions involves the following:

- (1) We propose a federated learning framework that overcomes privacy and robustness issues with reduced communication cost, especially for high-dimensional models. The convergence analysis and empirical results show that our framework maintains competitive accuracy while reducing communication and computation cost significantly.
- (2) To protect the privacy of local gradients, we propose a novel dot product aggregation protocol. Directly using packed Shamir secret sharing for dot product calculation can result in information leakage. Our dot product aggregation algorithm addresses this issue by ensuring that the server only learns the single value of the dot product and not other information about the local updates.
- (3) Our framework guarantees the secrecy and integrity of secret shares for a server-mediated network model using encryption and signature techniques.

2 Literature Review

In this section, we summarize the related works in defense strategy against poisoning attackers and robust privacy-preserving FL.

Defense against Poisoning Attacks: various robust aggregation rules have been proposed to defend against poisoning attacks. KRUM selects the benign updates based on the pairwise Euclidean distances between the gradients [8]. Yin et al. [43] proposed two robust coordinate-wise aggregation rules that computes the median and trimmed mean at each dimension, respectively. Bulyan [18] selects a set of gradients using Byzantine-resilient algorithm such as KRUM, and then aggregates the updates with trimmed mean. RSA [40] adds a regularization term to the objective function such that the local models are encouraged to be similar to the global model. In FLTrust [11], the server maintains a model on its clean root dataset and computes the cosine similarity to detect the malicious users. The aforementioned defense strategies analyze the individual gradients in plaintext, and thus are susceptible to privacy leakage.

Robust Privacy-Preserving FL: to enhance privacy and resist poisoning attacks, several frameworks have integrated homomorphic encryption (HE) with existing defense techniques. Based on Paillier cryptosystem, PEFL [30] calculated the Pearson correlation coefficient between coordinate-wise medians and local gradients to detect malicious users. PBFL [35] used cosine similarity to identify poisonous gradients and adopted fully homomorphic encryption (FHE) to ensure security. ShieldFL [31] computed cosine similarity between encrypted gradients with poisonous baseline for Byzantine-tolerance aggregation. The above approaches inherit the costly computation overhead of HE. Furthermore, they rely two non-colluding parties to perform secure computation and thus might be vulnerable to privacy leakage. Secure Multi-party Computation (SMC) is an alternative to address the privacy concern. To the best of our knowledge, BREa [41] is the first work that

developed Byzantine robust FL framework using verifiable Shamir secret sharing. However, their method suffers high communication complexity of SMC and high computation complexity of KRUM aggregation protocol.

This paper explores the integration of SMC with defense strategy against poisoning attacks. We develop a framework that reduces communication cost, employs a more efficient aggregation rule and guarantees the security for a server-mediated model.

3 Problem Formulation and Background

3.1 Problem Statement

We assume that the server trains a model \mathbf{w} with N mobile clients in a federated learning setting. All parties are assumed to be computationally bounded. Each client holds a local dataset $\{D_i\}_{i \in [N]}$, and the server owns a small, clean root dataset D_0 . The objective is to optimize the expected risk function:

$$F(\mathbf{w}) = \min_{\mathbf{w}} \mathbb{E}_{D \sim \chi} L(D, \mathbf{w}) \quad (1)$$

where $L(D, \mathbf{w})$ is an empirical loss function given dataset D .

In federated learning, the server aggregates local gradients \mathbf{g}_i^t to obtain global gradient \mathbf{g}^t for model update:

$$\mathbf{g}^t = \sum_{i \in S} \eta_i^t \mathbf{g}_i^t, \quad \mathbf{w}^t = \mathbf{w}^{t-1} - \gamma^t \mathbf{g}^t \quad (2)$$

where η_i is the weight of client i , γ^t is the learning rate, and S is the set of selected clients.

3.2 Adversary Model

We consider two types of users, i.e., honest users and malicious users. The definitions of honest and malicious users are given as follows.

Definition 3.1 (Honest Users). A user u is honest if and only if u honestly submits its local gradient g_u , where g_u is the true gradients trained on its local dataset D_u .

Definition 3.2 (Malicious Users). A user u is malicious if and only if u is manipulated by an adversary who launches model poisoning attack by submitting poisonous gradients g_u^* .

Server aims to infer users' information with two types of attacks, i.e., passive inference and active inference attack. In passive inference attack, the server tries to infer users' sensitive information by the intermediate result it receives from the user or eardrops during communication. In active inference attack, the server would manipulate certain users' messages to obtain the private values of targeted users.

3.3 Design Goals

We aim to design a federated learning system with three goals.

Privacy. Under federated learning, users might still be concerned about the information leakage from individual gradients. To protect privacy, the server shouldn't have access to local update of any user. Instead, the server learns only the aggregation weights and global gradients, ensuring that individual user data remains protected.

Robustness. We aim to design a method resilient to model poisoning attack, meaning that the model accuracy should be within a reasonable range under malicious clients.

Efficiency. Our framework should maintain computation and communication efficiency even if it's operated on high dimensional vectors.

3.4 Cryptographic Primitives

In this section we briefly describe cryptographic primitives for our framework. For more details refer to Appendix C.

Packed Shamir Secret Sharing: this study uses a generalization of Shamir secret sharing scheme [39], known as "packed secret-sharing" that allows to represent multiple secrets by a single polynomial [15]. A degree- d ($d \geq l - 1$) packed Shamir sharing of $\mathbf{s} = (s_1, s_2, \dots, s_l)$ stores the l secrets at a polynomial $f(\cdot)$ of degree at most d . The secret sharing scheme requires $d + 1$ shares for reconstruction, and any $d - l + 1$ shares reveals no information of the secret.

Key Exchange: the framework relies on Diffie–Hellman key exchange protocol [14] that allows two parties to establish a secret key securely.

Symmetric Encryption: Symmetric encryption guarantees the secrecy for communication between two parties [13]. The encryption and decryption are conducted with the same key shared by both communication partners.

Signature Scheme: To ensure the integrity and authenticity of message, we adopt a UF-CMA secure signature scheme [24, 23].

4 Framework

4.1 Overview

Figure 3 depicts the overall framework of our robust federated learning algorithm. The algorithm consists of four rounds:

Round 1: each client receives the server update g_0 , computes their updates normalized by g_0 , and distributes the secret shares of their updates to other clients.

Round 2: each client computes the local shares of partial dot product for gradient norm and cosine similarity, and conduct secret re-sharing on the local shares.

Round 3: each client obtains final shares of partial dot product for gradient norm and cosine similarity, and transmit the shares to server. Then the server would verify the gradient norm, recover cosine similarity, and compute the trust score for each client.

Round 4: on receiving the trust score from the server, each client conducts robust aggregation on the secret shares locally, and transmit the secret shares of aggregated gradient to the server. The server finally reconstructs the aggregation on the secret shares.

To address increased information leakage caused by packed secret sharing, we design a dot product aggregation protocol to sum up the dot product over sub-groups of elements. Refer to Appendix E for the algorithm to perform robust federated learning.

4.2 Normalization and Quantization

To limit the impact of attackers, we follow [11] to normalize each local gradient based on the server model update:

$$\bar{\mathbf{g}}_i = \frac{\|\mathbf{g}_0\|}{\|\mathbf{g}_i\|} \cdot \mathbf{g}_i \quad (3)$$

where \mathbf{g}_i is the local gradient of the i th client, and \mathbf{g}_0 is the server gradient obtain from clean root data.

Each client performs local gradient normalization, and the server validates if the updates are truly normalized. The secret sharing scheme operates over finite field \mathbb{F}_p for some large prime number p , and thus the user should quantize their normalized update $\bar{\mathbf{g}}_i$. The quantization poses challenge on normalization verification, as $\|\bar{\mathbf{g}}_i\|$ might not be exactly equal to $\|\mathbf{g}_0\|$ after being converted into finite field.

To address this issue, we define the following rounding function:

$$Q(x) = \begin{cases} \lfloor qx \rfloor / q, & x \geq 0 \\ (\lfloor qx \rfloor + 1) / q, & x < 0 \end{cases} \quad (4)$$

where $\lfloor qx \rfloor$ is the largest integer less than or equal to qx .

Therefore, the server could verify that $\|\bar{\mathbf{g}}_i\| \leq \|\mathbf{g}_0\|$, which is ensured by the quantization method.

4.3 Robust Aggregation Rule

Consistent with FLTrust[11], our framework conducts robust aggregation using the cosine similarity between users' and server's updates. The trust score of user i is:

$$TS_i = \max\left(0, \frac{\langle \mathbf{g}_i, \mathbf{g}_0 \rangle}{\|\mathbf{g}_i\| \|\mathbf{g}_0\|}\right) = \max\left(0, \frac{\langle \bar{\mathbf{g}}_i, \mathbf{g}_0 \rangle}{\|\mathbf{g}_0\|^2}\right) \quad (5)$$

where we clip the negative cosine similarity to zero to avoid the impact of malicious clients.

The global gradient is then aggregated by:

$$\mathbf{g} = \frac{1}{\sum_{i=1}^N TS_i} \sum_{i=1}^N TS_i \cdot \bar{\mathbf{g}}_i \quad (6)$$

Finally, we use the gradient to update the global model:

$$\mathbf{w} \leftarrow \mathbf{w} - \gamma \mathbf{g} \quad (7)$$

Our framework leverages the robust aggregation rule consistent with FLTrust due to its advantages including low computation cost, the absence of a requirement for prior knowledge about number of poisoners, defend against majority number of poisoners, and compatibility with Shamir Secret Sharing. Appendix D details the comparison between FLTrust and existing robust aggregation rules.

4.4 Verifiable Packed Secret Sharing

The core idea of packed secret sharing is to encode l secrets within a single polynomial. Consequently, the secrets shares of local updates generated by each user would reduce from NM to NM/l . By selecting $l = O(N)$, the per-user communication cost at secret sharing stage can be decreased to $O(M+N)$. We assume that the prime number P is large enough such that $P > \max\{N\|\mathbf{g}_0\|, \|\mathbf{g}_0\|^2\}$ to avoid overflow.

One issue with secret sharing is that a malicious client may send invalid secret shares, i.e., shares that are not evaluated at the same polynomial function, to break the training process. To address this issue, the framework utilizes the verifiable secret sharing scheme from [22], which generates constant size commitment to improve communication efficiency. We construct the verifiable secret shares for both local gradients and partial dot products described in Section 4.5. During verifiable packed secret sharing, the user would send the secret shares \mathbf{s} , commitment \mathcal{C} , and witness w_l to other users. A commitment is a value binding to a polynomial function $\phi(x)$, i.e., the underlying generator of the secret shares, without revealing it. A witness allows others to verify that the secret share s_l is generated at l of the polynomial (see Appendix F for more details).

4.5 Dot Product Aggregation

Directly applying packed secret sharing may increase the risk of information leakage when calculating cosine similarity and gradient norm. In the example provided by Figure 1, the gradient vectors are created as secret shares by packing l secret into a polynomial function. Following the local similarity computations by each client, the server can reconstruct the element-wise product between the two gradients, which makes it easy to recover the user's gradient \tilde{g}_i from the reconstructed metric. On the other hand, our proposed protocol ensures that only the single value of dot product is released to the server. Based on this, we introduce a term *partial dot product*, or *partial cosine similarity (norm square)* depending on the input vectors, defined as followed:

Partial dot product represents the multiple dot products of several subgroups of elements from input vectors rather than a single dot product value.

Another related concept is *final dot product*, referring to the single value of dot products between two vectors. For example, given two vectors $\mathbf{v}_1 = (2, -1, 4, 5, 6, 3)$ and $\mathbf{v}_2 = (1, 2, 0, 3, -2, 1)$, the reconstructed *partial dot product* could be $(0, 15, -9)$ if we pack 2 elements into a secret share, while the *final dot product* is 6. If each client directly uploads the shares from local dot product computation, the server would reconstruct a vector of partial cosine similarity (norm square) and thus learn more gradient information. To ensure that the server only has access to final cosine similarity

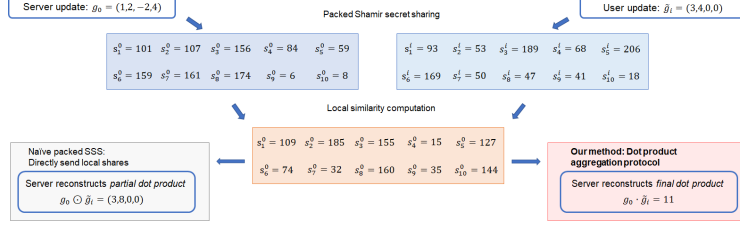


Figure 1: Cosine similarity computation on packed secret sharing

(norm square), we design a dot product aggregation algorithm based on secret re-sharing that allows the users to sum up the dot products over subgroups.

Suppose that the user i create a packed secret sharing $\mathbf{V}^i = \{v_{jk}^i\}_{j \in [N], k \in [\lceil m/l \rceil]}$ of $\tilde{\mathbf{g}}_i = (g_1^i, g_2^i, \dots, g_M^i)$, by packing each l elements into a secret. On receiving the secret shares, each user j can compute the vectors $\mathbf{cs}^j = (cs_1^j, cs_2^j, \dots, cs_N^j)$ and $\mathbf{nr}^j = (nr_1^j, nr_2^j, \dots, nr_N^j)$:

$$cs_k^j = \sum_l v_{jl}^k \cdot v_{jl}^0, nr_k^j = \sum_l v_{jl}^k \cdot v_{jl}^k \quad (8)$$

, where cs_k^j and nr_k^j denotes the shares of partial cosine similarity and partial gradient norm square for user k .

The partial cosine similarity (or gradient norm square) could be further aggregated by the below procedure in four steps.

Step 1: Secret resharing of partial dot product. Each user i could construct the verifiable packed secret shares of \mathbf{cs}^i (or \mathbf{nr}^j) by representing p secrets on a polynomial:

$$\mathbf{S}^i = \begin{pmatrix} s_{11}^i & \dots & s_{1\lceil N/p \rceil}^i \\ \vdots & \ddots & \vdots \\ s_{N1}^i & \dots & s_{N\lceil N/p \rceil}^i \end{pmatrix} \quad (9)$$

where s_{jk}^i denotes the share sent to user j for the k^{th} group of elements in vector \mathbf{cs}^i (or \mathbf{nr}^j). By choosing $p = O(N)$, each user will generate $O(N)$ secret shares.

Step 2: Disaggregation on re-combination vector. After distributing the secret shares, each user i receive a re-combination vector $\mathbf{s}_{ik} = (s_{ik}^1, s_{ik}^2, \dots, s_{ik}^N)$ for $k \in [\lceil N/p \rceil]$. Since we pack l elements for the secret shares of partial dot product, this step aims to transform the \mathbf{s}_{ik} into l vectors, with each vector representing one element. For each $j \in [l]$, user i locally computes:

$$\tilde{\mathbf{h}}_{jk}^i = \mathbf{s}_{ik} B_{e_j}^{-1} \mathit{Chop}_d \quad (10)$$

where B_{e_j} is an n by n matrix whose (i, k) entry is $(\alpha_k - e_j)^{i-1}$, and Chop_d is an n by n matrix whose (i, k) entry is 1 if $1 \leq i = k \leq d$ and 0 otherwise.

Step 3: Aggregation along packed index. The new secrets are summed up along $j \in [l]$ at client side:

$$\mathbf{h}_k^i = \sum_{j=1}^l \tilde{\mathbf{h}}_{jk}^i \quad (11)$$

Step 4: Decoding for final secret shares. User i can derive the final secret shares x_k^i by recovering from $\mathbf{h}_k^i = (h_{k1}^i, h_{k2}^i, \dots, h_{kN}^i)$ using Reed-Solomon decoding. Noted that $\{x_k^i\}_{k \in [\lceil N/p \rceil]}$ becomes a packed secret share of dot products of degree d (see Appendix G). Therefore, the server could recover the cosine similarity (or gradient norm square) for all users on receiving the final shares from sufficient users.

4.6 Secret Sharing over Insecure Channel

This framework relies on a server-mediated communication channel for the following reasons: (1) it's challenging for mobile clients to establish direct communication with each other and authenticate

other devices; (2) a server could act as central coordinator to ensure that all clients have access to the latest model. On the other hand, the secret sharing stage requires to maintain the privacy and integrity of secret shares.

To protect the secrecy of message, we utilize key agreement and symmetric encryption protocol. The clients establish the secret keys with each other through Diffie–Hellman key exchange protocol. During secret sharing, each client u uses the common key k_{uv} to encrypt the message sent to client v , and client v could decrypt the cyphertext with the same key.

Another concern is that the server may falsify the messages transmitted between clients. Signature scheme is adopted to prevent the active attack from server. We assume that all clients receive their private signing key and public signing keys of all other clients from a trusted third party. Each client i generate a signature σ_i along with the message m , and other clients verify the message using client i 's public key d_i^{PK} .

5 Theoretical Analysis

5.1 Complexity Analysis

In this section, we analyze the per iteration complexity for N selected clients, and model dimension of M , and summarize the complexity in table 1. More details about the complexity analysis can be referred to Appendix H. One important observation is that the communication complexity of our protocol reduces from $O(MN + N)$ to $O(M + N)$. Furthermore, the server-side computation overhead is reduced to $O((M + N) \log^2 N \log \log N)$, benefiting from the efficient aggregation rule and packed secret sharing. It should be noted that while the BERA protocol has similar server communication complexity, it makes an unrealistic assumption that users can share secrets directly with each other, thereby saving the server's overhead.

Table 1: Complexity summary of RFLPA and BERA

	RFLPA		BERA	
	Computation	Communication	Computation	Communication
Server	$O((M + N) \log^2 N \log \log N)$	$O((M + N)N)$	$O((N^2 + MN) \log^2 N \log \log N)$	$O(MN + N^2)$
User	$O((M + N^2) \log^2 N)$	$O((M + N))$	$O(MN \log^2 N + MN^2)$	$O(MN + N)$

5.2 Security Analysis

The security analysis is conducted for algorithm 3. Given a security parameter κ , a server S , and any subsets of users \mathcal{U} , let $\text{REAL}_{\mathcal{C}}^{\mathcal{U},t,\kappa}$ be a random variable representing the joint view of parties in $\mathcal{C} \subseteq \mathcal{U} \cup S$ where the threshold is set to t , and \mathcal{U}_i be the subset of respondents at round i such that $\mathcal{U} \supseteq \mathcal{U}_1 \supseteq \mathcal{U}_2 \supseteq \mathcal{U}_3 \supseteq \mathcal{U}_4$. We show that the joint view of any group of parties from \mathcal{C} with users less than t can be simulated given the inputs of clients in that group, trust score $\{TS_j\}_{j \in \mathcal{U}_1}$, and global gradient \mathbf{g} . In other words, *the server learns no information about clients' input except the global gradient and trust score.*

Theorem 5.1 (Security against active server and clients). *There exists a PPT simulator SIM such that for all $t \leq K - L$, $|\mathcal{C} \setminus \{S\}| < t$, the output of SIM is computationally indistinguishable from the output of $\text{REAL}_{\mathcal{C}}^{\mathcal{U},t,\kappa}$:*

$$\text{REAL}_{\mathcal{C}}^{\mathcal{U},t,\kappa}(\mathbf{x}_{\mathcal{U}}) \equiv \text{SIM}_{\mathcal{C}}^{\mathcal{U},t,\kappa}(\mathbf{x}_{\mathcal{U}}) \quad (12)$$

where " \equiv " represents computationally indistinguishable.

5.3 Correctness against Malicious Users

In this section, we show that our protocol executes correctly under the following attacks of malicious users: (1) sending invalid secret shares; (2) sending shares from incorrect computation of 6, 8, 10, or 11. Note that adversaries may also create shares from arbitrary gradients, and we left the discussion of such attack to Section 5.4.

The first attack arises when the user doesn't generate shares from the same polynomial. Such attempt is prevented by verifiable secret sharing that allows for the verification of share validity by testing 18.

The second attack could be addressed by Reed-Solomon codes. For a degree- d packed Shamir secret sharing with n shares, the Reed-Solomon decoding algorithm could recover the correct result with E errors and S erasures as long as $S + 2E + d + 1 \leq n$.

5.4 Convergence Analysis

Theorem 5.2. *Suppose Assumption K.1, K.2, K.3 in Appendix hold. For arbitrary number of malicious clients, the difference between the global model \mathbf{w}^t learnt by our algorithm and the optimal \mathbf{w}^* is bounded. Formally, we have the following inequality with probability at least $1 - \delta$:*

$$\|\mathbf{w}^t - \mathbf{w}^*\| \leq (1 - \rho)^t \|\mathbf{w}^0 - \mathbf{w}^*\| + 12\gamma\Delta_1 + \frac{\gamma\sqrt{d}}{q} \quad (13)$$

where $\rho = 1 - (\sqrt{1 - \mu^2/(4L_g^2)} + 24\gamma\Delta_2 + 2\gamma L)$, $\Delta_1 = \nu_1 \sqrt{\frac{2}{|D_0|}} \sqrt{d \log 6 + \log(3/\delta)}$, $\Delta_2 = \nu_2 \sqrt{\frac{2}{|D_0|}} \sqrt{d \log \frac{18L_2}{\nu_2} + \frac{1}{2}d \log \frac{|D_0|}{d} + \log\left(\frac{6\nu_2^2 r \sqrt{D_0}}{\alpha_2 \nu_1 \delta}\right)}$, $L_2 = \max\{L, L_1\}$.

Remark 5.3. $\gamma\sqrt{d}/q$ is the noise caused by the quantization process in our algorithm.

6 Experiments

6.1 Experimental Setup

Dataset: we use three standard datasets to evaluation the performance of RFLPA: MNIST [28], FashionMNIST (F-MNIST) [42], and CIFAR-10 [26]. MNIST and F-MNIST are trained on the neural network classification model composed of two convolutional layers and two fully connected layers, while CIFAR-10 is trained and evaluated with a ResNet-9 [19] model.

Attacks: we simulate two types of poisoning attacks: gradient manipulation attack (untargeted) and label flipping attack (targeted). Under gradient manipulation attack, the malicious users generate arbitrary gradients from normal distribution of mean 0 and standard deviation 200. For label flipping attack, the adversaries flip the label from l to $P - l - 1$, where P is the number of classes. We consider the proportion of attackers from 0% to 30%.

6.2 Experiment Results

6.2.1 Accuracy Evaluation

We compare our proposed method with several FL frameworks: FedAvg [25], Bulyan [18], Trim-mean [43], local differential privacy (LDP) [36], central differential privacy (CDP) [36], and BREA [41]. Refer to Table 5 for the coarse-grained comparison between RFLPA and the baselines. Noted that PEFL, PBFL, and ShieldFL is not included in the accuracy comparison because: (i) The security of the three schemes relies on the assumption that the server would not collude with a third-party during training, which is vulnerable in real life. (ii) The three frameworks entail significant computation costs, rendering their implementation in real-life scenarios impractical (see Appendix L.7.1). Table 2 summarizes the accuracies for different methods under the two attacks.

When defense strategy is not implemented, the accuracies of FedAvg decrease as the proportion of attackers increases, with a more significant performance drop observed under gradient manipulation attacks. Benefited from the trust benchmark, our proposed framework, RFLPA, demonstrates more stable performance for up to 30% adversaries compared to other baselines. In the absence of attackers, our method achieves slightly lower accuracies than FedAvg, with an average decrease of 2.84%, 4.38% and 3.46%, respectively, for MNIST, F-MNIST, and CIFAR-10 dataset. (see Appendix L.5, L.6 and L.8 for more analysis.)

6.2.2 Overhead Analysis

To verify the effectiveness of our framework on reducing overhead, we compare the per-iteration communication and computation cost for BREA and RFLPA in Figure 2. For each experiment we set

the degree as $0.4N$ and encode $0.1N$ elements within a polynomial. (See Appendix L.7 for more analysis)

The left-most graph presents the overhead with different participating client size using the 1.6M parameter model described in Section 6.1. For $M \gg N$, the per-client communication complexity for RFLPA remains stable at around 82.5MB, regardless of user size. Conversely, BREa exhibits linear scalability with the number of participating clients. Our framework reduces the communication cost by over 75% compared with BREa.

The second left graph examines the communication overhead for varying model dimensions with 2,000 participating clients. RFLPA achieves a much lower per-client cost than BREa by leveraging packed secret sharing, leading to a 99.3% reduction in overhead.

The right two figures presents the computation cost under varying client size using a MNIST classifier with 1.6M parameters. Benefiting from the packed VSS, RFLPA reduces both the user and server computation overhead by over 80% compared with BREa.

Table 2: Accuracy under different proportions of attackers. The values denote the mean \pm standard deviation of the performance.

Proportion of Attackers		Gradient Manipulation				Label Flipping			
		No	10%	20%	30%	No	10%	20%	30%
FedAvg	MNIST	0.98 \pm 0.0	0.46 \pm 0.1	0.40 \pm 0.1	0.32 \pm 0.0	0.98 \pm 0.0	0.96 \pm 0.0	0.92 \pm 0.0	0.82 \pm 0.0
	F-MNIST	0.88 \pm 0.0	0.55 \pm 0.0	0.51 \pm 0.0	0.45 \pm 0.1	0.88 \pm 0.0	0.82 \pm 0.0	0.73 \pm 0.0	0.69 \pm 0.0
	CIFAR-10	0.76 \pm 0.3	0.14 \pm 0.2	0.13 \pm 0.8	0.13 \pm 0.2	0.76 \pm 0.3	0.72 \pm 1.1	0.68 \pm 2.7	0.59 \pm 0.8
Bulyan	MNIST	0.98 \pm 0.0	0.92 \pm 0.0	0.89 \pm 0.0	0.87 \pm 0.0	0.98 \pm 0.0	0.91 \pm 0.0	0.90 \pm 0.0	0.87 \pm 0.0
	F-MNIST	0.86 \pm 0.0	0.73 \pm 0.0	0.71 \pm 0.1	0.69 \pm 0.0	0.86 \pm 0.0	0.76 \pm 0.0	0.70 \pm 0.1	0.68 \pm 0.0
	CIFAR-10	0.77 \pm 1.0	0.73 \pm 0.8	0.45 \pm 1.2	0.27 \pm 0.6	0.77 \pm 1.0	0.72 \pm 0.2	0.62 \pm 1.8	0.40 \pm 0.9
Trim-mean	MNIST	0.98 \pm 0.0	0.95 \pm 0.0	0.93 \pm 0.0	0.91 \pm 0.0	0.98 \pm 0.0	0.95 \pm 0.0	0.92 \pm 0.0	0.90 \pm 0.0
	F-MNIST	0.86 \pm 0.0	0.81 \pm 0.0	0.74 \pm 0.0	0.71 \pm 0.0	0.86 \pm 0.0	0.78 \pm 0.0	0.74 \pm 0.0	0.73 \pm 0.0
	CIFAR-10	0.76 \pm 1.0	0.57 \pm 2.1	0.51 \pm 1.1	0.47 \pm 2.2	0.76 \pm 1.0	0.71 \pm 1.3	0.68 \pm 0.7	0.56 \pm 1.1
LDP	MNIST	0.87 \pm 0.1	0.13 \pm 0.0	0.10 \pm 0.0	0.10 \pm 0.0	0.87 \pm 0.1	0.87 \pm 0.3	0.83 \pm 1.2	0.77 \pm 2.1
	F-MNIST	0.74 \pm 0.1	0.59 \pm 0.4	0.53 \pm 1.2	0.12 \pm 0.0	0.74 \pm 0.1	0.63 \pm 0.5	0.62 \pm 0.2	0.59 \pm 1.2
	CIFAR-10	0.14 \pm 0.2	0.14 \pm 0.2	0.12 \pm 0.3	0.12 \pm 0.1	0.14 \pm 0.2	0.14 \pm 0.2	0.14 \pm 0.3	0.13 \pm 0.1
CDP	MNIST	0.96 \pm 0.0	0.96 \pm 0.0	0.95 \pm 0.0	0.94 \pm 0.0	0.96 \pm 0.0	0.96 \pm 0.0	0.95 \pm 0.3	0.91 \pm 0.2
	F-MNIST	0.83 \pm 0.1	0.51 \pm 0.1	0.41 \pm 0.0	0.34 \pm 0.1	0.83 \pm 0.1	0.81 \pm 0.5	0.79 \pm 0.0	0.78 \pm 0.7
	CIFAR-10	0.71 \pm 1.2	0.12 \pm 0.5	0.12 \pm 0.3	0.12 \pm 0.3	0.71 \pm 1.2	0.68 \pm 0.7	0.66 \pm 1.5	0.63 \pm 1.3
BREa	MNIST	0.94 \pm 0.0	0.93 \pm 0.0	0.93 \pm 0.0	0.93 \pm 0.0	0.94 \pm 0.0	0.94 \pm 0.0	0.93 \pm 0.0	0.93 \pm 0.0
	F-MNIST	0.84 \pm 0.0	0.83 \pm 0.0	0.82 \pm 0.0	0.81 \pm 0.0	0.84 \pm 0.0	0.84 \pm 0.0	0.82 \pm 0.0	0.81 \pm 0.0
	CIFAR-10	0.70 \pm 1.0	0.69 \pm 1.1	0.68 \pm 1.9	0.68 \pm 0.7	0.70 \pm 1.0	0.70 \pm 2.2	0.67 \pm 0.9	0.65 \pm 2.7
RFLPA	MNIST	0.96 \pm 0.0	0.96 \pm 0.0	0.95 \pm 0.0	0.95 \pm 0.0	0.96 \pm 0.0	0.96 \pm 0.0	0.95 \pm 0.0	0.95 \pm 0.0
	F-MNIST	0.84 \pm 0.0	0.84 \pm 0.0	0.83 \pm 0.0	0.82 \pm 0.0	0.84 \pm 0.0	0.83 \pm 0.0	0.83 \pm 0.0	0.82 \pm 0.0
	CIFAR-10	0.74 \pm 2.3	0.70 \pm 1.8	0.70 \pm 1.9	0.69 \pm 1.8	0.74 \pm 2.3	0.71 \pm 1.7	0.70 \pm 1.6	0.69 \pm 0.8

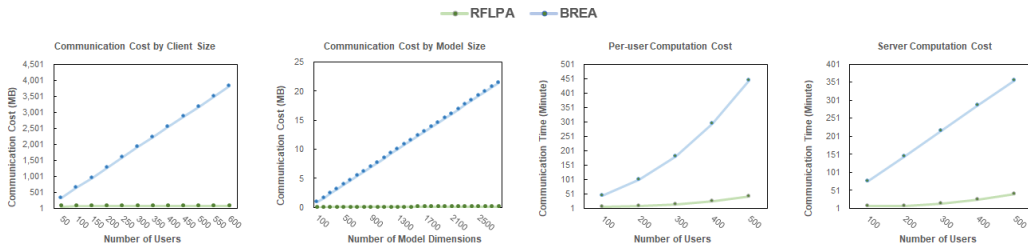


Figure 2: Per-iteration communication (left two) and computation cost (right two).

7 Conclusion

This paper proposes RFLPA, a robust privacy-preserving FL framework with SecAgg. Our framework leverages verifiable packed Shamir secret sharing to compute the cosine similarity between user and server update and conduct robust aggregation. We design a secret re-sharing algorithm to address the increased information leakage concern, and utilize encryption and signature techniques to ensure the security over server-mediated channel. Our approach achieves the reduced per-user communication overhead of $O(M + N)$. The empirical study demonstrates that: (1) RFLPA achieves competitive accuracies for up to 30% poisoning adversaries compared with state-of-the-art defense methods. (2) The communication cost and computation cost for RFLPA is significantly lower than BREa by over 75% under the same FL settings.

References

- [1] Gagan Aggarwal, Nina Mishra, and Benny Pinkas. “Secure computation of the k th-ranked element”. In: *Advances in Cryptology-EUROCRYPT 2004: International Conference on the Theory and Applications of Cryptographic Techniques, Interlaken, Switzerland, May 2-6, 2004. Proceedings 23*. Springer. 2004, pp. 40–55.
- [2] Menezes Alfred, Vanstone Scott, et al. *Handbook of applied cryptography*. 1997.
- [3] Eugene Bagdasaryan et al. “How to backdoor federated learning”. In: *International Conference on Artificial Intelligence and Statistics*. PMLR. 2020, pp. 2938–2948.
- [4] James Henry Bell et al. “Secure single-server aggregation with (poly) logarithmic overhead”. In: *Proceedings of the 2020 ACM SIGSAC Conference on Computer and Communications Security*. 2020, pp. 1253–1269.
- [5] Mihir Bellare and Chanathip Namprempre. “Authenticated encryption: Relations among notions and analysis of the generic composition paradigm”. In: *Advances in Cryptology—ASIACRYPT 2000: 6th International Conference on the Theory and Application of Cryptology and Information Security Kyoto, Japan, December 3–7, 2000 Proceedings 6*. Springer. 2000, pp. 531–545.
- [6] Luisa Bentivogli et al. “The Fifth PASCAL Recognizing Textual Entailment Challenge.” In: *TAC 7.8 (2009)*, p. 1.
- [7] Arnaud Berlioz et al. “Applying differential privacy to matrix factorization”. In: *Proceedings of the 9th ACM Conference on Recommender Systems*. 2015, pp. 107–114.
- [8] Peva Blanchard et al. “Machine learning with adversaries: Byzantine tolerant gradient descent”. In: *Advances in neural information processing systems 30 (2017)*.
- [9] Keith Bonawitz et al. “Practical secure aggregation for privacy-preserving machine learning”. In: *proceedings of the 2017 ACM SIGSAC Conference on Computer and Communications Security*. 2017, pp. 1175–1191.
- [10] Dan Boneh and Xavier Boyen. “Short signatures without random oracles”. In: *Advances in Cryptology-EUROCRYPT 2004: International Conference on the Theory and Applications of Cryptographic Techniques, Interlaken, Switzerland, May 2-6, 2004. Proceedings 23*. Springer. 2004, pp. 56–73.
- [11] Xiaoyu Cao et al. “FLTrust: Byzantine-robust Federated Learning via Trust Bootstrapping”. In: *ISOC Network and Distributed System Security Symposium (NDSS)*. 2021.
- [12] Di Chai et al. “Secure federated matrix factorization”. In: *IEEE Intelligent Systems 36.5 (2020)*, pp. 11–20.
- [13] Hans Delfs et al. “Symmetric-key encryption”. In: *Introduction to cryptography: principles and applications (2007)*, pp. 11–31.
- [14] Whitfield Diffie and Martin E Hellman. “New directions in cryptography”. In: *Democratizing Cryptography: The Work of Whitfield Diffie and Martin Hellman*. 2022, pp. 365–390.
- [15] Matthew Franklin and Moti Yung. “Communication complexity of secure computation”. In: *Proceedings of the twenty-fourth annual ACM symposium on Theory of computing*. 1992, pp. 699–710.
- [16] Matt Fredrikson, Somesh Jha, and Thomas Ristenpart. “Model inversion attacks that exploit confidence information and basic countermeasures”. In: *Proceedings of the 22nd ACM SIGSAC conference on computer and communications security*. 2015, pp. 1322–1333.
- [17] Shuhong Gao. “A new algorithm for decoding Reed-Solomon codes”. In: *Communications, information and network security (2003)*, pp. 55–68.
- [18] Rachid Guerraoui, Sébastien Rouault, et al. “The hidden vulnerability of distributed learning in byzantium”. In: *International Conference on Machine Learning*. PMLR. 2018, pp. 3521–3530.
- [19] Kaiming He et al. “Deep residual learning for image recognition”. In: *Proceedings of the IEEE conference on computer vision and pattern recognition*. 2016, pp. 770–778.
- [20] Ling Huang et al. “Adversarial machine learning”. In: *Proceedings of the 4th ACM workshop on Security and artificial intelligence*. 2011, pp. 43–58.
- [21] Peter Kairouz, Ziyu Liu, and Thomas Steinke. “The distributed discrete gaussian mechanism for federated learning with secure aggregation”. In: *International Conference on Machine Learning*. PMLR. 2021, pp. 5201–5212.

- [22] Aniket Kate, Gregory M Zaverucha, and Ian Goldberg. “Constant-size commitments to polynomials and their applications”. In: *Advances in Cryptology-ASIACRYPT 2010: 16th International Conference on the Theory and Application of Cryptology and Information Security, Singapore, December 5-9, 2010. Proceedings 16*. Springer. 2010, pp. 177–194.
- [23] Jonathan Katz. *Digital signatures*. Vol. 1. Springer, 2010.
- [24] Ravneet Kaur and Amandeep Kaur. “Digital signature”. In: *2012 International Conference on Computing Sciences*. IEEE. 2012, pp. 295–301.
- [25] Jakub Konečný et al. “Federated learning: Strategies for improving communication efficiency”. In: *arXiv preprint arXiv:1610.05492* (2016).
- [26] Alex Krizhevsky et al. “Learning multiple layers of features from tiny images”. In: (2009).
- [27] Hsiang-Tsung Kung. *Fast evaluation and interpolation*. Carnegie-Mellon University. Department of Computer Science, 1973.
- [28] Yann LeCun et al. “Gradient-based learning applied to document recognition”. In: *Proceedings of the IEEE* 86.11 (1998), pp. 2278–2324.
- [29] Hector Levesque, Ernest Davis, and Leora Morgenstern. “The winograd schema challenge”. In: *Thirteenth international conference on the principles of knowledge representation and reasoning*. 2012.
- [30] Xiaoyuan Liu et al. “Privacy-enhanced federated learning against poisoning adversaries”. In: *IEEE Transactions on Information Forensics and Security* 16 (2021), pp. 4574–4588.
- [31] Zhuoran Ma et al. “ShieldFL: Mitigating model poisoning attacks in privacy-preserving federated learning”. In: *IEEE Transactions on Information Forensics and Security* 17 (2022), pp. 1639–1654.
- [32] Brendan McMahan et al. “Communication-efficient learning of deep networks from decentralized data”. In: *Artificial intelligence and statistics*. PMLR. 2017, pp. 1273–1282.
- [33] H Brendan McMahan et al. “Federated learning of deep networks using model averaging”. In: *arXiv preprint arXiv:1602.05629 2* (2016).
- [34] Luca Melis et al. “Exploiting unintended feature leakage in collaborative learning”. In: *2019 IEEE symposium on security and privacy (SP)*. IEEE. 2019, pp. 691–706.
- [35] Yinbin Miao et al. “Privacy-preserving Byzantine-robust federated learning via blockchain systems”. In: *IEEE Transactions on Information Forensics and Security* 17 (2022), pp. 2848–2861.
- [36] Mohammad Naseri, Jamie Hayes, and Emiliano De Cristofaro. “Local and central differential privacy for robustness and privacy in federated learning”. In: *arXiv preprint arXiv:2009.03561* (2020).
- [37] Thông T Nguyễn et al. “Collecting and analyzing data from smart device users with local differential privacy”. In: *arXiv preprint arXiv:1606.05053* (2016).
- [38] V Sanh. “DistilBERT, a distilled version of BERT: smaller, faster, cheaper and lighter.” In: *Proceedings of Thirty-third Conference on Neural Information Processing Systems (NIPS2019)*. 2019.
- [39] Adi Shamir. “How to share a secret”. In: *Communications of the ACM* 22.11 (1979), pp. 612–613.
- [40] Junyu Shi et al. “Challenges and approaches for mitigating byzantine attacks in federated learning”. In: *2022 IEEE International Conference on Trust, Security and Privacy in Computing and Communications (TrustCom)*. IEEE. 2022, pp. 139–146.
- [41] Jinhyun So, Başak Güler, and A Salman Avestimehr. “Byzantine-resilient secure federated learning”. In: *IEEE Journal on Selected Areas in Communications* 39.7 (2020), pp. 2168–2181.
- [42] Han Xiao, Kashif Rasul, and Roland Vollgraf. “Fashion-mnist: a novel image dataset for benchmarking machine learning algorithms”. In: *arXiv preprint arXiv:1708.07747* (2017).
- [43] Dong Yin et al. “Byzantine-robust distributed learning: Towards optimal statistical rates”. In: *International Conference on Machine Learning*. PMLR. 2018, pp. 5650–5659.
- [44] Ligeng Zhu, Zhijian Liu, and Song Han. “Deep leakage from gradients”. In: *Advances in neural information processing systems* 32 (2019).

A Notation Table

Table 3: Notation table.

NOTATION	DESCRIPTION	NOTATION	DESCRIPTION
\mathbf{w}	Model parameter	\mathbf{g}	Gradients
D, D_0, D_i	Dataset	η_i	Aggregation weight
γ^t	Learning rate	S	Set of participation clients
N	Participating client size	M	Model dimension
\mathbf{V}^i, v_{jk}^i	Packed secret shares for gradients	TS_i	Trust score
l	# of secrets packed at a polynomial for gradient	p	# of secrets packed at a polynomial for shares of partial dot product
\mathbf{cs}^j, cs_k^j	Shares of partial cosine similarity	\mathbf{nr}^j, nr_k^j	Shares of partial gradient norm square
\mathbf{S}^i, s_{jk}^i	Packed secret shares of \mathbf{cs}^j or \mathbf{nr}^j	$\tilde{\mathbf{h}}_k^i$	Secret shares disaggregated along packed index
x_k^i	Packed secret share of dot product	\mathbf{h}_k^i	Secret shares aggregated along packed index
e_i	Pre-determined secret point	α_i	Pre-selected elements for secret sharing
B_{e_j}	n by n matrix whose (i, k) entry is $(\alpha_k - e_j)^{i-1}$	$Chop_d$	n by n matrix whose (i, k) entry is 1 if $1 \leq i = k \leq d$ and 0 otherwise

B Overview of RFLPA

Figure 3 depicts the overview of RFLPA.

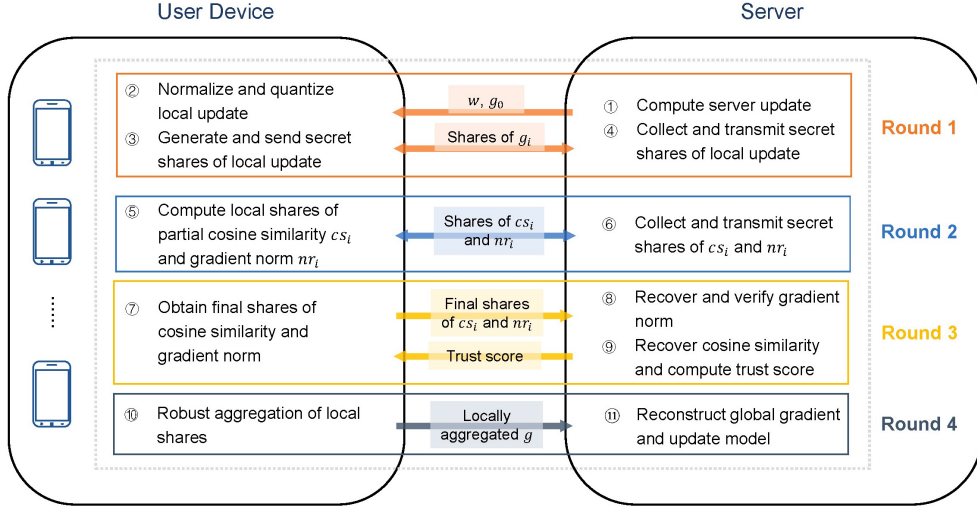


Figure 3: Overall framework

C Details of Cryptographic Primitives

C.1 Packed Shamir Secret Sharing

The operations of Packed Shamir Secret Sharing performed on a finite field \mathbb{F}_P for some prime number P . Denote $\{e_i\}_{i \in [l]}$ as the pre-determined secret point, and $\{\alpha_i\}_{i \in [d]}$ as the pre-selected elements for secret sharing. To share the secrets $\mathbf{g} = (g_1, g_2, \dots, g_l)$, the user can generate a degree- d polynomial function:

$$\phi(x) = q(x) \prod_{i=1}^l (x - e_i) + \sum_{i=1}^l g_i L_i(x) \quad (14)$$

where $q(x)$ is a random degree- $d - l$ polynomial, and $L_i(x)$ is the Lagrange polynomial $\frac{\prod_{j \neq i} (x - e_j)}{\prod_{j \neq i} (e_i - e_j)}$.

The shares sent to player j is generated by:

$$s_j = \phi(\alpha_j) \quad (15)$$

We use $\langle \mathbf{g} \rangle_d$ to denote the degree- d packed secret shares of vector \mathbf{g} . The following properties holds for the packed sharing scheme:

- $\langle \alpha \mathbf{x} + \beta \mathbf{y} \rangle_d = \alpha \langle \mathbf{x} \rangle_d + \beta \langle \mathbf{y} \rangle_d$
- $\langle \mathbf{x} * \mathbf{y} \rangle_{d_1+d_2} = \langle \mathbf{x} \rangle_{d_1} * \langle \mathbf{y} \rangle_{d_2}$

C.2 Key Exchange

Diffie–Hellman key exchange protocol consists of the following algorithms:

- *Generate parameters:* $pp = \mathbf{GenParam}(sp)$ set up the parameters, including prime number and primitive root, according to the security parameter.
- *Key generation:* $(s_i^{SK}, s_i^{PK}) = \mathbf{KEGen}(pp)$ generates the private-public key pairs for user i .
- *Key derivation:* $s_{ij} = \mathbf{KEAgree}(s_i^{SK}, s_j^{PK})$ outputs the shared secret key between user i and j .

C.3 Symmetric Encryption

The symmetric encryption scheme consists of the following algorithms:

- *Encryption:* $c = \mathbf{Enc}(m, k)$ encrypts message m to cyphertext c using key k .
- *Decryption:* $m = \mathbf{Dec}(c, k)$ reverses cyphertext c to message m using key k .

To ensure correctness, we require that $m = \mathbf{Dec}(\mathbf{Enc}(m, k), k)$. For security, the encryption scheme should be indistinguishability under a chosen plaintext attack (IND-DPA) and integrity under ciphertext-only attack (INT-CTXT) [5].

C.4 Signature Scheme

The UF-CMA secure signature scheme that consists of a tuple of algorithms ($\mathbf{Gen}, \mathbf{Sign}, \mathbf{Verify}$):

- *Key generation:* Based on the security parameter sp , $(d^{SK}, d^{PK}) = \mathbf{SigGen}(sp)$ returns the private-public key pairs.
- *Signing algorithm:* $\sigma = \mathbf{Sign}(d^{SK}, m)$ generates a signature σ with secret key and message as input.
- *Signature verification:* $\mathbf{Verify}(d^{PK}, m, \sigma)$ takes as input the public key, a message and a signature, and returns 1 if the signature is valid and 0 otherwise.

To proof the security of the signature scheme, we show that no adversary can forge a valid signature on an arbitrary message. Denote a UF-CMA secure signature scheme as $\text{DS} = (\mathbf{k}, \mathbf{Sign}, \mathbf{Verify})$, where k is the security parameter. The UF-CMA advantage of an adversary A is defined as $\text{Adv}_{\text{DS}}(A, k) = \mathbb{P}(\text{Exp}_{\text{DS}}^{\text{uf-cma}}(A, k) = 1)$, where $\text{Exp}_{\text{DS}}^{\text{uf-cma}}(A, k)$ represents the experiments conducted by adversary A to produce a signature, and $\text{Exp}_{\text{DS}}^{\text{uf-cma}}(A, k) = 1$ means that A produced a valid signature. In a UF-CMA secure signature scheme, no probabilistic polynomial time (PPT) adversary is able to produce a valid signature on an arbitrary message with more than negligible probability. In other words, for all PPT adversaries A , there exists a negligible function ϵ such that $\text{Adv}_{\text{DS}}(A, k) \leq \epsilon(k)$.

D Comparison between Byzantine-robust aggregation rules

To provide justification for our algorithm’s utilization of FLTrust as the aggregation rule, we summarize the existing Byzantine-robust aggregation rules along four dimensions: (i) computation complexity, (ii) whether the algorithm needs prior knowledge about the number of poisoners, (iii) maximum number of poisoners, (iv) whether the algorithm is compatible with Shamir Secret Sharing (SSS).

Table 4: Comparison between Byzantine-robust aggregation rules.

	Computation complexity	Need prior knowledge about # of poisoners	# of poisoners	Compatible with SSS
KRUM	$O(N^2(M + \log N))$	Yes	< 50%	Yes
Bulyan	$O(N^2M)$	Yes	< 25%	No
Trim-mean	$O(MN \log N)$	Yes	< 50%	No
FLTrust	$O(MN)$	No	< 100%	Yes

Among these dimensions, FLTrust demonstrates clear advantages over other robust aggregation rules:

- *Low computation cost:* for a system with N users and M model size, the computation cost of FLTrust is $O(MN)$, lower than existing methods that grow quadratically with N .
- *No need of prior knowledge about number of poisoners:* the server does not need to know the number of malicious clients in advance to conduct robust aggregation.
- *Defend against majority number of poisoners:* benefiting from the trusted root of clean dataset at the server, the aggregation rule we adopted can return robust result even when the number of poisoners is above 50%.
- *Compatible with Shamir Secret Sharing (SSS):* the method we adopted is compatible with the SSS algorithm. While for Bulyan and Trim-mean, there are some non-linear operations not supported by SSS.

E Algorithm of RFLPA

This section presents the our algorithm to conduct robust federated learning with secure aggregation.

Algorithm 1 RFLPA

Input: Local dataset D_i of clients $i \in [N]$, root dataset D_0 at server, number of iterations T , security parameter κ .
Output: Global model \mathbf{w}^T
 Clients set up encryption and signature key pairs $(c_i^{PK}, c_i^{SK}), (d_i^{PK}, d_i^{SK}) \leftarrow \text{SetupKeys}(N, \kappa)$ for $i \in [N]$.
 Server initialize global model \mathbf{w}^0
for $t \in [1, T]$ **do**
 Server conduct local update with root data, compute update norm $\|\mathbf{g}_0\|$, and create packed secret shares \mathbf{v}_0 .
 Each clients from \mathcal{U}_t download global model \mathbf{w}^{t-1} , corresponding shares of \mathbf{v}_0 , and $\|\mathbf{g}_0\|$.
 Server obtain gradients $\mathbf{g} \leftarrow \text{RobustSecAgg}(\mathcal{U}_t, \mathbf{w}^{t-1}, \mathbf{v}_0, \|\mathbf{g}_0\|)$
 Server update global model $\mathbf{w}^t \leftarrow \mathbf{w}^{t-1} - \gamma^t \mathbf{g}$
end for

Suppose that user i create a packed secret shares \mathbf{s} of \mathbf{g} with polynomial $\phi(x)$. Providing κ security, the user sets up generator ψ and secret key α , and also outputs the public key $(\psi, \psi^\alpha, \dots, \psi^{\alpha^d})$ for a degree d polynomial. To make the secret shares verifiable, the user broadcasts a commitment to the function:

$$\mathcal{C} = \psi^{\phi(\alpha)} \tag{16}$$

Algorithm 2 SetupKeys

Input: number of clients N , security parameter κ .

Output: key pairs $\{(d_i^{PK}, d_i^{SK})\}_{i \in [N]}$;
secret keys $\{k_{ij}\}_{i,j \in [N]}$.

Each user $i \in [N]$ receive their signing key d_i^{SK} from the trusted third party, as well as the verification keys d_j^{PK} of all users $j \in [N]$.

Each user $i \in [N]$ generate key pairs $(s_i^{SK}, s_i^{PK}) = \mathbf{KEGen}(sp)$, and create signature $\sigma_i = \mathbf{Sign}(d_i^{PK}, s_i^{SK})$.

Users $i \in [N]$ send $(s_i^{PK} || \sigma_i)$, public key along with signature, to the server.

Server distribute $\{(s_i^{PK} || \sigma_i)\}_{i \in [N]}$ to all users.

Each user i asserts that $\mathbf{Verify}(d_i^{PK}, s_j^{PK}, \sigma_j) = 1$, and compute $k_{ij} = \mathbf{KEAgree}(s_i^{SK}, s_j^{PK})$ for $j \in [N] \setminus i$.

F Verifiable Packed Secret Sharing

For each secret s_l , user i computes a witness sent to the corresponding client in a private channel:

$$w_l = \psi^{(\phi(\alpha) - \phi(l)) / (\alpha - l)} \quad (17)$$

After receiving the commitment and witness, user l can verify the secret by checking:

$$e(\mathcal{C}, \psi) = e(w_l, \psi^\alpha / \psi^l) e(\psi, \psi)^{\phi(l)} \quad (18)$$

where $e(\cdot)$ denotes a symmetric bilinear pairing.

The correctness and secrecy of the protocol are guarantee by the discrete logarithm (DL) [2], t -polynomial Diffie-Hellman (t -polyDH) [22], and t -Strong Diffie-Hellman (t -SDH) [10] assumptions.

G Explanation of Secret Re-sharing

For $m \in [[N/p]]$, the shares of secret $cs_{(m-1)p+k}^i$ for some $k \in [p]$ can be represented as:

$$(s_{1m}^i \dots s_{Nm}^i) = (cs_{(m-1)p+k}^i \theta_1 \dots \theta_d 0 \dots 0) \times B_{e_k} \quad (19)$$

where $\{\theta_j\}_{j \in [d]}$ are random integers.

Hence, the user side computation of 10 is the same as:

$$\begin{aligned} & \begin{pmatrix} s_{1m}^1 & \dots & s_{1m}^N \\ \vdots & & \vdots \\ s_{Nm}^1 & \dots & s_{Nm}^N \end{pmatrix} B_{e_j}^{-1} \mathbf{Chop}_d B_{e_j'} = B_{e_k}^T \\ & \times \begin{pmatrix} cs_{(m-1)p+k}^1 & \dots & cs_{(m-1)p+k}^N \\ \vdots & & \vdots \end{pmatrix} B_{e_j}^{-1} \mathbf{Chop}_d \end{aligned} \quad (20)$$

The aggregation of new secret and reconstruction of $\{x_m^j\}$ is equivalent to taking the first column of:

$$\begin{aligned} & B_{e_k}^T \begin{pmatrix} cs_{(m-1)p+k}^1 & \dots & cs_{(m-1)p+k}^N \\ \vdots & & \vdots \end{pmatrix} \\ & \times (B_{e_1}^{-1} + \dots + B_{e_l}^{-1}) \mathbf{Chop}_d \end{aligned} \quad (21)$$

Since cs^j is a packed secret share of the partial cosine similarity, it follows that:

$$(cs_h^1 \dots cs_h^N) B_{e_j}^{-1} \mathbf{Chop}_d = \left(\sum_{(j-1)l < i \leq jl} \bar{g}_{hi} g_{0i} \dots \right) \quad (22)$$

, meaning that the first elements gives the partial cosine similarity.

Therefore, the final shares sent to server $\{x_m^j\}$ can be formulated as:

$$(x_m^1 \dots x_m^N) = \left(\sum_i \bar{g}_{m(p-1)+h,i} g_{0i} \theta_1 \dots \theta_d 0 \dots \right) B_{e_h} \quad (23)$$

, for $h \in (m(p-1), mp]$. Therefore, the server could retrieve the dot product by Reed-Solomon decoding, which is equivalent to multiplying $\{B_{e_h}^{-1}\}_{h \in (m(p-1), mp]}$ and obtaining the first element.

Algorithm 3 RobustSecAgg

Input: Set of active clients in current iteration \mathcal{U}_0 , global parameters \mathbf{w} downloaded from server, packed secret shares of server update \mathbf{v}_0 , norm of server update $\|\mathbf{g}_0\|$.

Output: Global aggregated gradient \mathbf{g}

Round 1:

Client i :

- Generate local gradient \mathbf{g}_i
- Generate packed secrets $\{\mathbf{s}_{ij}\}_{j \in \mathcal{U}_0}$, commitments \mathcal{C} and witness $\{\mathbf{v}_{ij}\}_{j \in \mathcal{U}_0}$ for \mathbf{g}_i from 15, 16, and 17, encrypt $\mathbf{c}_{ij} = \mathbf{Enc}(\mathbf{s}_{ij} \parallel \mathbf{v}_{ij}, k_{ij})$, and create signature $\sigma_{ij} = \mathbf{Sign}(d_i^{SK}, \mathbf{c}_{ij} \parallel \mathcal{C})$ for $j \in [N] \setminus i$
- Send $(\mathcal{C} \parallel \{\mathbf{c}_{ij}\}_{j \in [N] \setminus i} \parallel \{\sigma_{ij}\}_{j \in [N] \setminus i})$ to the server

Server:

- Collect messages from at least K clients (denote \mathcal{U}_1 the set of all respondents).
- Send $(\mathcal{C} \parallel \{\mathbf{c}_{ij}\}_{i \in \mathcal{U}_1 \setminus j} \parallel \{\sigma_{ij}\}_{i \in \mathcal{U}_1 \setminus j})$ to client j for $j \in \mathcal{U}_1$.

Round 2:

Client i :

- Receive $(\mathcal{C} \parallel \{\mathbf{c}_{ji}\}_{j \in \mathcal{U}_1 \setminus i} \parallel \{\sigma_{ji}\}_{j \in \mathcal{U}_1 \setminus i})$ from server, and assert that $\mathbf{Verify}(d_j^{PK}, \mathbf{c}_{ji} \parallel \mathcal{C}, \sigma_{ji}) = 1$.
- Recover $(\{\mathbf{s}_{ji}\}_{j \in \mathcal{U}_1 \setminus i}, \{\mathbf{v}_{ji}\}_{j \in \mathcal{U}_1 \setminus i}) = \mathbf{Dec}(\mathbf{c}_{ji}, k_{ji})$, and verify the secret shares $\{\mathbf{s}_{ji}\}_{j \in \mathcal{U}_1 \setminus i}$ by testing 18.
- Compute local shares of partial norm $\{nr_j^i\}_{j \in \mathcal{U}_1}$ and partial cosine similarity $\{cs_j^i\}_{j \in \mathcal{U}_1}$ from 8.
- Construct packed secret shares $\{\mathbf{s}'_{ik}\}_{k \in \mathcal{U}_1}$, commitments \mathcal{C} , and witness $\{\mathbf{v}'_{ik}\}_{k \in \mathcal{U}_1}$ for $(\{nr_j^i\}_{j \in \mathcal{U}_1}, \{cs_j^i\}_{j \in \mathcal{U}_1})$, encrypt $\mathbf{c}'_{ik} = \mathbf{Enc}(\mathbf{s}'_{ik} \parallel \mathbf{v}'_{ik}, k_{ik})$, and create signature $\sigma'_{ik} = \mathbf{Sign}(d_i^{SK}, \mathbf{c}'_{ik} \parallel \mathcal{C})$ for $k \in [N] \setminus i$
- Send $(\mathcal{C} \parallel \{\mathbf{c}'_{ij}\}_{j \in [N] \setminus i} \parallel \{\sigma'_{ij}\}_{j \in [N] \setminus i})$ to the server

Server:

- Collect messages from at least K clients (denote \mathcal{U}_2 the set of all respondents).
- Send $(\mathcal{C} \parallel \{\mathbf{c}'_{ij}\}_{i \in \mathcal{U}_2 \setminus j} \parallel \{\sigma'_{ij}\}_{i \in \mathcal{U}_2 \setminus j})$ to client j for $j \in \mathcal{U}_2$.

Round 3:

Client i :

- Receive $(\mathcal{C} \parallel \{\mathbf{c}'_{ji}\}_{j \in \mathcal{U}_2 \setminus i} \parallel \{\sigma'_{ji}\}_{j \in \mathcal{U}_2 \setminus i})$ from server, and assert that $\mathbf{Verify}(d_j^{PK}, \mathbf{c}'_{ji} \parallel \mathcal{C}, \sigma'_{ji}) = 1$.
- Recover $(\{\mathbf{s}'_{ji}\}_{j \in \mathcal{U}_2 \setminus i}, \{\mathbf{v}'_{ji}\}_{j \in \mathcal{U}_2 \setminus i}) = \mathbf{Dec}(\mathbf{c}'_{ji}, k_{ji})$, and verify the secret shares $\{\mathbf{s}'_{ji}\}_{j \in \mathcal{U}_2 \setminus i}$ by testing 18.
- Obtain the final share of norm $\{\overline{nr}_j^i\}_{j \in |\mathcal{U}_1|/p}$ and cosine similarity $\{\overline{cs}_j^i\}_{j \in |\mathcal{U}_1|/p}$ from 10, 11, and Reed-Solomon decoding.
- Send $(\{\overline{nr}_j^i\}_{j \in |\mathcal{U}_1|/p}, \{\overline{cs}_j^i\}_{j \in |\mathcal{U}_1|/p})$ to the server.

Server:

- Collect messages from at least K clients (denote \mathcal{U}_3 the set of all respondents).
- Recover $\{\|\mathbf{g}_j\|^2\}_{j \in \mathcal{U}_1}$ using Reed-Solomon decoding, and assert that $\|\mathbf{g}_j\|^2 \leq \|\mathbf{g}_0\|^2, \forall j \in \mathcal{U}_1$.
- Recover $\{\langle \mathbf{g}_i, \mathbf{g}_0 \rangle\}_{j \in \mathcal{U}_1}$ using Reed-Solomon decoding, and compute the trust score $\{TS_j\}_{j \in \mathcal{U}_1}$ from 5.
- Broadcast the trust score $\{TS_j\}_{j \in \mathcal{U}_1}$ to all users $i \in \mathcal{U}_3$.

Round 4:

Client i :

- Compute local aggregation $\langle \mathbf{g} \rangle_i$ from 6, and send to the server.

Server:

- Collect messages from at least K clients.
 - Recover \mathbf{g} using Reed-Solomon decoding.
-

H Details of Complexity Analysis

User computation: User's computation cost can be broken as: (1) generating packed secret shares of update ($O(M + N) \log^2 N$) complexity [27]); (2) computing shares of partial gradient norm square and cosine similarity ($O(M + N)$) complexity); (3) creating packed secret shares of partial gradient norm square and cosine similarity ($O(N \log^2 N)$) complexity); (4) deriving final secret shares of

gradient norm square and cosine similarity ($O(N^2 \log^2 N)$ complexity). Therefore, each user's computation cost is $O((M + N^2) \log^2 N)$.

User communication: User's communication cost can be broken as: (1) downloading parameters from server ($O(M)$ messages); (2) sending and receiving secret shares of gradient ($O((M, N))$ messages); (3) sending and receiving secret shares of partial gradient norm square and cosine similarity ($O(N)$ messages); (4) sending final shares of gradient norm square and cosine similarity ($O(1)$ messages); (5) receiving trust scores from the server ($O(N)$ messages); (6) sending shares of aggregated update to the server ($O(M/N + 1)$ messages). Hence, each user's communication cost is $O(M + N)$.

Server computation: The server's computation cost can be broken as: (1) recovering gradient norm square and cosine similarity by Reed-Solomon decoding ($O(N \log^2 N \log \log N)$ complexity [17]); (2) computing the trust score of each user ($O(N)$ complexity); (3) decoding the aggregated global gradient ($O(M + N) \log^2 N \log \log N$ complexity). Therefore, the server's computation cost is $O((M + N) \log^2 N \log \log N)$.

Server communication: The server's communication cost can be broken as: (1) distributing parameters to clients ($O(MN)$ messages); (2) sending and receiving secret shares of user update ($O((M + N)N)$ messages); (3) sending and receiving secret shares of partial gradient norm square and cosine similarity ($O(N^2)$ messages); (4) receiving final shares of gradient norm square and cosine similarity ($O(N)$ messages); (5) broadcasting trust scores to clients ($O(N^2)$ messages); (6) receiving shares of aggregated update from clients ($O(M + N)$ messages). Overall, the server's communication cost is $O((M + N)N)$.

I Proof of Theorem 5.1

Proof. We utilize the standard hybrid argument to prove the theorem. we define a PPT simulator SIM through a series of (polynomially many) subsequent to $\text{REAL}_C^{\mathcal{U}, t, \kappa}$, so that the view of \mathcal{C} in SIM is computationally indistinguishable from that in $\text{REAL}_C^{\mathcal{U}, t, \kappa}$.

Hyb₁: In the hybrid, each honest user from $\mathcal{U}_1 \setminus \mathcal{C}$ encrypts shares of a uniformly random vector, instead of the raw gradients. The properties of Shamir's secret sharing ensure that the distribution of any $|\mathcal{C} \setminus \{S\}| < t$ shares of raw gradients is identical to that of any equivalent length vector, and IND-CPA security guarantees that the view of server is indistinguishable in both cases. Hence, this hybrid is identical from the previous one.

Hyb₂: In the hybrid, the simulator aborts if \mathcal{C} provides any of the honest user i with a signature on j 's message, \mathbf{c}_{ji} , but the user couldn't produce the same signature given the public key (in round 2). The security of the signature scheme guarantees that this hybrid is indistinguishable from the previous one.

Hyb₃: In this hybrid, SIM aborts if any of the honest user i fails to verify the secret shares \mathbf{s}_{ji} from user j by checking 18. The DL, t -polyDH, and t -SDH assumptions guarantee that this hybrid is identical from the previous one.

Hyb₄: In the hybrid, each honest user from $\mathcal{U}_2 \setminus \mathcal{C}$ encrypts shares of a uniformly random vector rather than partial norm and cosine similarity. The properties of Shamir's secret and IND-CPA security ensure that this hybrid is indistinguishable from the previous one.

Hyb₅: In the hybrid, the simulator aborts if \mathcal{C} provides any of the honest user i with a signature on j 's message, \mathbf{c}'_{ji} , but the user couldn't produce the same signature given the j 's key (in round 3). Because of the security of the signature scheme, this hybrid is indistinguishable from the previous one.

Hyb₆: This hybrid is defined as Hyb₃, with the only difference that SIM verify the secret shares \mathbf{s}'_{ji} in round 3. This hybrid is indistinguishable from the previous one under DL, t -polyDH, and t -SDH assumptions.

The above changes do not modify the views seen by the colluding parties, and the hybrid doesn't make use of the honest users' input. Therefore, the output of SIM is computationally indistinguishable from the output of $\text{REAL}_C^{\mathcal{U}, t, \kappa}$, and this concludes the proof.

□

J Proof of Theorem 5.2

Denote $\bar{\mathbf{g}}^t = \sum_i \eta_i \bar{\mathbf{g}}_i$ be the aggregated gradients at iteration t .

Lemma J.1. *For arbitrary number of adversarial clients, the distance between $\bar{\mathbf{g}}^t$ and $\nabla F(\mathbf{w}^t)$ is bounded by:*

$$\|\bar{\mathbf{g}}^t - \nabla F(\mathbf{w}^t)\| \leq 3\|\mathbf{g}_0^t - \nabla F(\mathbf{w}^t)\| + 2\|\nabla F(\mathbf{w}^t)\| + \frac{\sqrt{d}}{q} \quad (24)$$

Proof. It follows that:

$$\begin{aligned} \|\bar{\mathbf{g}}^t - \nabla F^t(\mathbf{w})\| &= \left\| \sum_i \eta_i \bar{\mathbf{g}}_i - \nabla F^t(\mathbf{w}) \right\| \\ &= \left\| \sum_i \eta_i \bar{\mathbf{g}}_i - \bar{\mathbf{g}}_0 + \bar{\mathbf{g}}_0 - \mathbf{g}_0 + \mathbf{g}_0 - \nabla F^t(\mathbf{w}) \right\| \\ &\leq \left\| \sum_i \eta_i \bar{\mathbf{g}}_i - \bar{\mathbf{g}}_0 \right\| + \|\bar{\mathbf{g}}_0 - \mathbf{g}_0\| + \|\mathbf{g}_0 - \nabla F^t(\mathbf{w})\| \\ &\leq \sum_i \eta_i \|\bar{\mathbf{g}}_i\| + \|\bar{\mathbf{g}}_0\| + \|\bar{\mathbf{g}}_0 - \mathbf{g}_0\| + \|\mathbf{g}_0 - \nabla F^t(\mathbf{w})\| \\ &\stackrel{(a)}{\leq} 2\|\mathbf{g}_0\| + \frac{\sqrt{d}}{q} + \|\mathbf{g}_0 - \nabla F^t(\mathbf{w})\| \\ &\leq 3\|\mathbf{g}_0 - \nabla F^t(\mathbf{w})\| + 2\|\nabla F^t(\mathbf{w})\| + \frac{\sqrt{d}}{q} \end{aligned} \quad (25)$$

where (a) is because $\sum_i \eta_i = 1$, $\|\bar{\mathbf{g}}_i\| \leq \|\mathbf{g}_0\|$, and $\|\bar{\mathbf{g}}_0\| \leq \|\mathbf{g}_0\|$. □

Lemma J.2. *Under Assumption K.1, we have the following bound at iteration t :*

$$\|\mathbf{w}^t - \mathbf{w}^* - \gamma \nabla F(\mathbf{w}^t)\| \leq \sqrt{1 - \mu^2/(4L_g^2)} \|\mathbf{w}^t - \mathbf{w}^*\| \quad (26)$$

Proof. Refer to lemma 2 in [11] for the proof. □

Lemma J.3. *Suppose Assumption K.1, K.2, K.3 holds. For any $\delta \in (0, 1)$, if $\Delta_1 \leq \nu_1^2/\alpha_1$, $\Delta_2 \leq \nu_2^2/\alpha_2$, we have:*

$$P \{ \|\mathbf{g}_0 - \nabla F(\mathbf{w})\| \leq 8\Delta_2 \|\mathbf{w} - \mathbf{w}^* + 4\Delta_1\| \} \geq 1 - \delta \quad (27)$$

for any $\mathbf{w} \in \Theta \subset \{ \mathbf{w} : \|\mathbf{w} - \mathbf{w}^*\| \leq r\sqrt{d} \}$ given some positive number r .

Proof. Refer to lemma 4 in [11] for the proof. □

Proof of Theorem 5.2: Given the lemmas above, we can proceed to prove Theorem 5.2. We have:

$$\begin{aligned} \|\mathbf{w} - \mathbf{w}^*\| &\leq \|\mathbf{w}^{t-1} - \gamma \nabla F(\mathbf{w}^{t-1}) - \mathbf{w}^*\| + \gamma \|\bar{\mathbf{g}}^t - \nabla F(\mathbf{w}^t)\| \\ &\leq \|\mathbf{w}^{t-1} - \gamma \nabla F(\mathbf{w}^{t-1}) - \mathbf{w}^*\| + 3\gamma \|\mathbf{g}_0^t - \nabla F(\mathbf{w}^t)\| \\ &\quad + 2\gamma \|\nabla F(\mathbf{w}^t)\| + \frac{\gamma \sqrt{d}}{q} \\ &\leq \left(\sqrt{1 - \mu^2/(4L^2)} + 24\gamma \Delta_2 + 2\gamma L \right) \|\mathbf{w}^{t-1} - \mathbf{w}^*\| \\ &\quad + 12\gamma \Delta_1 + \frac{\gamma \sqrt{d}}{q} \end{aligned} \quad (28)$$

Therefore, with probability at least $1 - \delta$, it follows that:

$$\|\mathbf{w}^t - \mathbf{w}^*\| \leq (1 - \rho)^t \|\mathbf{w}^0 - \mathbf{w}^*\| + 12\gamma \Delta_1 + \frac{\gamma \sqrt{d}}{q} \quad (29)$$

K Assumptions for convergence analysis 5.4

Assumption K.1. The expected risk function $F(\mathbf{w})$ is μ -strongly convex and L -smooth for any $\mathbf{w}, \bar{\mathbf{w}}$:

$$\begin{aligned} F(\bar{\mathbf{w}}) &\geq F(\mathbf{w}) + \langle \nabla F(\mathbf{w}), \bar{\mathbf{w}} - \mathbf{w} \rangle + \frac{\mu}{2} \|\bar{\mathbf{w}} - \mathbf{w}\|^2 \\ \|\nabla F(\mathbf{w}) - \nabla F(\bar{\mathbf{w}})\| &\leq L \|\bar{\mathbf{w}} - \mathbf{w}\| \end{aligned} \quad (30)$$

Moreover, the empirical loss function $L(D, \mathbf{w})$ is L_1 -smooth probabilistically. For any $\delta \in (0, 1)$, there exists an L_1 such that:

$$P \left\{ \sup_{\mathbf{w} \neq \bar{\mathbf{w}}} \frac{\|\nabla L(D, \mathbf{w}) - \nabla L(D, \bar{\mathbf{w}})\|}{\|\mathbf{w} - \bar{\mathbf{w}}\|} \leq L_1 \right\} \geq 1 - \frac{\delta}{3} \quad (31)$$

Assumption K.2. The root dataset D_0 and clients' local dataset $D_i (i = 1, 2, \dots, n)$ are sampled independently from distribution χ .

Assumption K.3. The gradients of the empirical loss function $\nabla L(D, \mathbf{w}^*)$ at the optimal model \mathbf{w}^* is bounded. Furthermore, $h(D, \mathbf{w}) = \nabla L(D, \mathbf{w}) - \nabla L(D, \mathbf{w}^*)$ is also bounded. Specifically, $\langle \nabla L(D, \mathbf{w}^*), \mathbf{v} \rangle$ and $\langle h(D, \mathbf{w}) - \mathbb{E}[h(D, \mathbf{w})], \mathbf{v} \rangle / \|\mathbf{w} - \mathbf{w}^*\|$ are sub-exponential for any unit vector \mathbf{v} . Formally, for $\forall |\lambda| \leq 1/\alpha_1, \forall |\lambda| \leq 1/\alpha_2, \mathbf{B} = \{\mathbf{v} : \|\mathbf{v}\| = 1\}$, it holds that:

$$\begin{aligned} \sup_{\mathbf{v} \in \mathbf{B}} \mathbb{E}[\exp(\lambda \langle \nabla L(D, \mathbf{w}^*), \mathbf{v} \rangle)] &\leq e^{\nu_1^2 \lambda^2 / 2} \\ \sup_{\mathbf{v} \in \mathbf{B}, \mathbf{w}} \mathbb{E} \left[\exp \left(\frac{\langle h(D, \mathbf{w}) - \mathbb{E}[h(D, \mathbf{w})], \mathbf{v} \rangle}{\|\mathbf{w} - \mathbf{w}^*\|} \right) \right] &\leq e^{\nu_2^2 \lambda^2 / 2} \end{aligned} \quad (32)$$

L Experiments

The experiments are conducted on a 16-core Ubuntu Linux 20.04 server with 64GB RAM and A6000 driver, where the programming language is Python.

L.1 Datasets

MNIST is a collection of handwritten digits, including 60,000 training and 10,000 testing images of 28×28 pixels. F-MNIST consists of 70,000 fashion images of size 28×28 and is split into 60,000 training and 10,000 testing samples. CIFAR-10 is natural dataset that includes 60,000 32×32 colour images in 10 classes, splitting into 50,000 training and 10,000 testing images.

L.2 FL configuration

both datasets are split among 10,000 users and select 100 users in each iteration. The server stores 200 clean samples as benchmark. We allow up to 20% clients to drop out in each round, and a maximum of 30% participating clients to collaborate with each other to reveal the secret. Therefore, we construct a secret sharing of degree 40, considering the doubling of degree during dot product computation, and pack each 10 elements into a secret.

L.3 Hyper-Parameters

The parameters are updated using Adaptive Moment Estimation (Adam) method with a learning rate of 0.01. Each accuracy reported in the tables is an average of 5 experiments, and each round of experiments runs for 200 iterations. Both LDP and CDP adopt privacy parameter $\epsilon = 3$ and $\delta = 0.0001$.

L.4 Comparison among Aggregation Frameworks

In Table 5 we summarize the comparison among aggregation frameworks along four dimensions:

- *Robustness against malicious users:* most algorithms provide certain level of robustness against malicious users. Local DP is not that effective in defending malicious users according to our experiment results.

- *Privacy Protection against server*: whether the framework protect user’s plaintext gradient against server. Only PEFL, PBFL, ShieldFL, BREA, and RFLPA achieves the goals of robustness and privacy simultaneously.
- *Collusion threshold during model training*: the server could obtain users’ plaintext gradients if it colludes with more than the given level of parties. PEFL, PBFL, and ShieldFL all rely on a trusted third-party during model training to protect users’ message. The collaboration between server and the trusted third-party could compromise user’s privacy.
- *MPC techniques*: the main multiparty computation techniques leveraged by the framework. PEFL, PBFL, and ShieldFL are based on homomorphic encryption (HE), and BREA and RFLPA are based on secret sharing.

Table 5: Corse-grained comparison among Aggregation Frameworks. “/” denotes non-applicable.

	Robustness against malicious users	Privacy Protection against server	Collusion threshold during model training	MPC techniques
FedAvg	Yes	No	/	/
Bulyan	Yes	No	/	/
Trim-mean	Yes	No	/	/
KRUM	Yes	No	/	/
Central DP	Yes	No	/	/
Local DP	Not effective	Yes	/	/
PEFL	Yes	Yes	1	HE (Paillier)
PBFL	Yes	Yes	1	HE (CKKS)
ShieldFL	Yes	Yes	1	HE (Paillier)
BREA	Yes	Yes	$O(N)$	Secret sharing
RFLPA	Yes	Yes	$O(N)$	Secret sharing

L.5 Accuracies over Iterations

Figure 4 demonstrates the impact of different iterations on test accuracies for RFLPA, BREA and FedAvg using the MNIST dataset. The results reveal that the RFLPA algorithm displays comparable convergence regardless of the existence of attackers, while FedAvg exhibits significantly inferior convergence when 30% attackers are present.

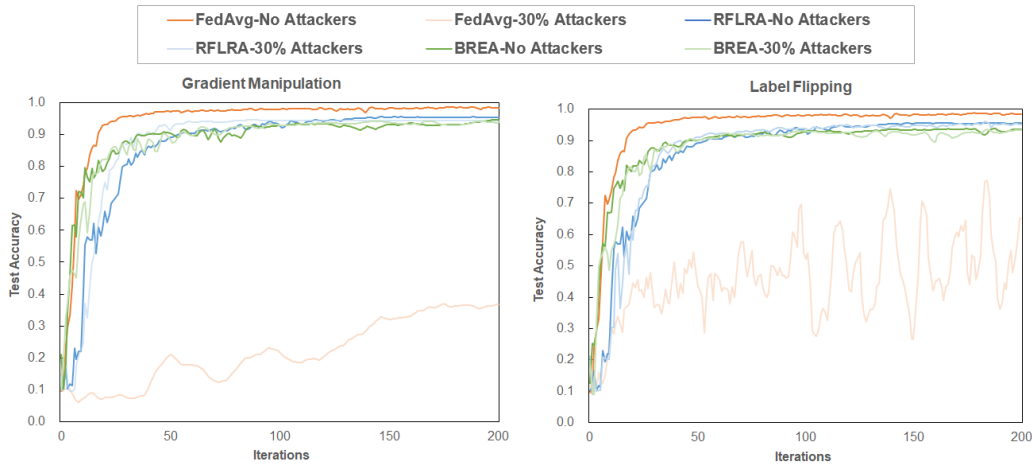


Figure 4: Test accuracy of RFLPA and FedAvg for different proportions of malicious users on MNIST dataset.

L.6 Performance on Natural Language Processing (NLP) Dataset

we evaluate the accuracy of our framework on two NLP datasets, Recognizing Textual Entailment (RTE) [6] and Winograd NLI (WNLI) [29], by finetuning a distillBERT model [38]. We present the performance for gradient manipulation attack in Table 6. The result demonstrates that for the two NLP datasets, RFLPA has robust accuracies in the presence of up to 30% attackers.

Table 6: Accuracies on NLP dataset under different proportions of attackers.

Proportion of Attackers	RTE				WNLI			
	No	10%	20%	30%	No	10%	20%	30%
FedAvg	0.599	0.509	0.487	0.462	0.619	0.563	0.437	0.437
BREA	0.584	0.592	0.570	0.567	0.592	0.592	0.577	0.563
RFLPA	0.596	0.582	0.582	0.577	0.619	0.592	0.592	0.563

L.7 Overhead Analysis

L.7.1 Computation Time between RFLPA and HE-based methods

To verify the practicability of RFLPA, we benchmark our framework with three HE-based methods, PEFL [30], PBFL [35], and ShieldFL [31]. Table 7 presents the per-iteration computation time using a MNIST classifier (1.6M parameters) for the three algorithms and RFLPA. It can be observed that it takes 1.5 to 6.5 day to run the three HE-based algorithms for only a single iteration, which renders them impractical for real-life deployment.

Table 7: Computation cost (in minutes) with varying client size.

Client size	Per-user Cost				Server Cost			
	100	200	300	400	100	200	300	400
RFLPA	3.41	11.44	24.51	42.60	6.68	8.46	15.00	26.47
PEFL	111.51	109.27	109.44	110.13	2156.20	6056.98	6785.71	9365.46
PBFL	12.65	12.58	12.73	12.63	1806.05	3598.54	5386.97	7193.64
ShieldFL	111.73	109.43	109.25	109.84	2192.48	6093.05	6809.60	9384.11

L.7.2 Ablation Study

Considering that RFLPA and BREA leverage different robust aggregation rule, we conducted ablation study to demonstrate that the reduction in overhead is attributed to the scheme design of RFLPA rather than the inherent advantages of the underlying aggregation rule. In particular, we replace the aggregation module in RFLPA with KRUM, and presents the per-iteration communication and computation cost, respectively, in Table 8 and 9. It can be observed that even with substituting the aggregation module with KRUM in our framework, there’s still notable reduction in the communication cost benefiting from the design of our secret sharing algorithm.

Table 8: Communication cost (in MB) per client with varying client size with MNIST classifier (1.6M parameters). RFLPA (KRUM) replaces the aggregation rule with KRUM in RFLPA.

Client size	300	400	500	600
RFLPA	82.51	82.52	82.53	82.54
BREA	1909.92	2544.45	3178.98	3813.51
RFLPA (KRUM)	79.58	82.25	85.68	89.87

L.8 Non-IID Setting

The previous experiments were conducted under the assumption that the local data of clients are independent and identically distributed (IID). To simulate the non-IID dataset, we adopted the setting in [32] by sorting the data based on their labels and dividing them into 10,000 subsets. Consequently, the local data owned by most clients consist of only one label.

Table 9: Computation cost (in minutes) with varying client size with MNIST classifier (1.6M parameters). RFLPA (KRUM) replaces the aggregation rule with KRUM in RFLPA.

Client size	Per-user Cost				Server Cost			
	100	200	300	400	100	200	300	400
RFLPA	3.41	11.44	24.51	42.60	6.68	8.46	15.00	26.47
BREA	44.73	101.39	182.27	294.27	75.85	145.30	216.96	287.22
RFLPA (KRUM)	13.60	35.56	46.48	75.78	31.77	34.04	39.76	62.81

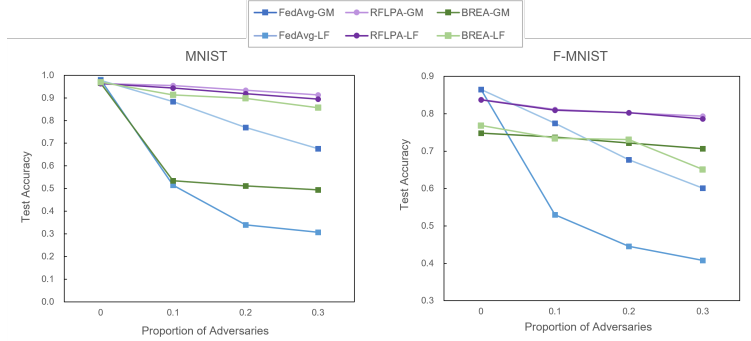


Figure 5: Test accuracy on non-IID dataset. GM stands for gradient manipulation attack, and LF stands for label flipping attack.

We compare the accuracy of RFLPA, BREA and FedAvg on non-IID dataset in Figure 5. The RFLPA demonstrates resilient performance against poisoning attacks, even when the dataset is distributed non-identically among clients.

M Discussion and Future Work

Collection of server data: one important assumption is that the server is required to collect a small, clean root dataset. Such collection is affordable for most organizations as the required dataset is of small size, e.g., 200 samples. According to theoretical analysis, the convergence is guaranteed when the root dataset is representative of the overall training data. Empirical evidence presented in [11] suggests that the performance of the global model is robust even when the root dataset diverges slightly from the overall training data distribution.

Compatibility with other defense strategies: RFLPA adopts a robust aggregation rule that computes the cosine similarity with server update. The framework can be easily generalized to distance-based method such as KRUM or multi-KRUM by substituting the robust aggregation module. However, extending the framework to rank-based defense methods may be more challenging. Existing SMC techniques for rank-based statistics requires $\log M$ rounds of communication, where M is the range of input values [1]. We leave the problem of communication-efficient rank-based robust FL to future work.

Differential privacy guarantee: differential privacy (DP) [37, 7] provides formal privacy guarantees to prevent information leakage. The combination of SMC and DP, also known as Distributed DP [21], reduces the magnitude of noise added by each user compared with pure local DP. However, adopting DP in the privacy-preserving robust FL framework is non-trivial, especially when bounding the privacy leakage of robustness metrics such as cosine similarity may sacrifice utility. We leave the problem of incorporating DP into the privacy-preserving robust FL framework to future work.